Dielectronic recombination from high-lying resonance states in H-like silicon, calcium, and iron

K. R. Karim and M. Ruesink
Department of Physics, Illinois State University, Normal, Illinois 61761

C. P. Bhalla
Department of Physics, Kansas State University, Manhattan, Kansas 66506
(Received 8 April 1992)

We have calculated dielectronic recombination (DR) rate coefficients for H-like silicon, calcium, and iron at plasma temperatures 0.1–10 keV. The calculation involves all DR processes $1s+\epsilon l_c \rightarrow (2lnl')^* \rightarrow 1sml''+\gamma$ with $n=2-\infty$. The effects of configuration interaction and spin-orbit coupling have been included for all states with $n \leq 8$; for higher-lying resonance states, the $1/n^3$ scaling was employed.

PACS number(s): 34.80.Kw, 52.70.La

I. INTRODUCTION

The dielectronic recombination (DR) of a H-like ion involves the following steps: (i) the capture of a free electron ϵl_c by an ion in the state $|i\rangle = |1s\,^2S_{1/2}\rangle$ with simultaneous excitation of the $1s$ electron to a higher orbit to form a doubly excited autoionizing state $|s\rangle = |2lnl'SLJ\rangle$ and (ii) the radiative decay of the state $|s\rangle = |2lnl'SLJ\rangle$ to a low-lying state $|f\rangle = |1sml''S'L'J'\rangle$, which is stable against autoionization. This process can schematically be represented as

$$1s+\epsilon l_c \rightarrow (2lnl')^* \rightarrow 1sml''+\gamma \ . \quad (1)$$

In a dielectronic recombination process, the kinetic energy of the free electron is transformed into photon energy which may be lost from the plasma. This constitutes an important energy-loss mechanism in high-temperature fusion plasmas. The dielectronic recombination also has significant effects on the ionization balance of the plasma, and, as such, this process was first recognized for its effects on the ionization equilibrium of the solar corona. Dielectronic recombination also leads to such prominent features as dielectronic satellite lines in the x-ray-emission spectra. These satellites provide a convenient method for spectroscopic diagnostics of laboratory and astrophysical plasmas.

Satellite spectra originating from dielectronic recombination of H-like ions have been observed in solar flares [1], laser-induced fusion devices [2], and in tokamaks [3,4]. The calculations on DR rates have generally been limited, however, to low-lying resonance states with $n \leq 4$, where n is the principal quantum number of the outermost electron of the intermediate resonance state $|s\rangle = |2lnl'SLJ\rangle$. Theoretical values of DR rate coefficients of H-like ions have been reported by Bitter *et al.* [4] ($Z=22$), Karim and Bhalla [5,6] ($Z=10,14,18,20,22,24,26,28$), Dubau *et al.* [7] ($Z=26$), and Chen [8] ($Z=24,54$). Calculations of DR cross sections for H-like carbon, oxygen, silicon, and sulfur have been reported recently by Pindzola, Badnell, and Griffin [9], who have used Hartree-Fock and Thomas-Fermi-Dirac-Amaldi wave functions to calculate DR cross sections. For calculating DR cross sections for $n>6$, they have extrapolated the matrix elements for electric dipole and electron-electron Coulomb interactions. Bitter *et al.* [4] used the Z-expansion technique and the multiconfiguration Thomas-Fermi model. We have earlier reported [5] on a calculation of DR rate coefficients of several H-like ions. Our calculation [5] was performed in the intermediate-coupling scheme with the inclusion of configuration interaction for states $|s\rangle = |2lnl'SLJ\rangle$ with $n=2$, 3, and 4 only; configuration average rates were used to calculate DR rates for $n=5$–8, and $1/n^3$ scaling was employed for $n>8$. We have recently reported [10,11] that the intensities of x-ray satellites originating from DR processes exhibit a rather more complex dependence on n than what the simple $1/n^3$ scaling law suggests. The purpose of the present paper is to report on a calculation of DR rates which explicitly includes all intermediate resonance states up to $n=8$ for H-like silicon, calcium, and iron.

II. THEORY

The intensity of a satellite line originating in the DR process as represented in Eq. (1) is given by

$$I_d(s \rightarrow f) = N_e N_i \alpha_d(s \rightarrow f) \ , \quad (2)$$

where N_e and N_i are, respectively, the densities of electrons and hydrogenlike ions in the initial state $|i\rangle = |1s\,^2S_{1/2}\rangle$ and $\alpha_d(s \rightarrow f)$ is the DR rate coefficients. Assuming a Maxwellian electron-energy distribution, the DR rate coefficients can be expressed as [12]

$$\alpha_d(s \rightarrow f) = \tfrac{1}{2}(2\pi\hbar^2/mkT_e)^{3/2} F_2^*(s \rightarrow f) \times \exp(-E_a/kT_e) \ , \quad (3)$$

where E_a is the Auger electron energy, k is Boltzmann's constant, T_e is the electron temperature, and $F_2^*(s \rightarrow f)$ are the satellite intensity factors. The satellite intensity factors are related to the ratio of the intensity of the satellite to the resonance line and are given by

$$F_2^*(s\to f)\equiv\frac{(2J_s+1)}{(2J_i+1)}\frac{\Gamma_a(s\to i)\Gamma_r(s\to f)}{\Gamma(s)}\ . \tag{4}$$

Here, J_s and J_i are, respectively, the total angular momentum quantum numbers of the autoionizing states $|s\rangle$ and the initial state $|i\rangle$, $\Gamma_a(s\to i)$ is the rate of autoionization of the state $|s\rangle$, $\Gamma_r(s\to f)$ is the rate for radiative transition, and $\Gamma(s)$ is the total rate for the state $|s\rangle$ in all possible radiative and autoionizing channels. The autoionization transition rates are given by

$$\Gamma_a=\frac{2\pi}{\hbar}\left|\left\langle\psi_f\left|\sum_{i>j}V_{ij}\right|\psi_i\right\rangle\right|^2\rho(E)\ , \tag{5}$$

where ψ_i and ψ_f are, respectively, the antisymmetrized many-electron wave functions of the initial and final states, $\rho(E)$ is the density of the final state, and $V_{ij}=1/r_{ij}$ is two the electron interaction operator.

The radiative transition probability is given by [13]

$$\Gamma_r(\gamma'J'-\gamma J)=\frac{4\omega^3}{3\hbar c^3}\frac{1}{2J+1}|\langle\gamma'J'\|D\|\gamma J\rangle|^2\ . \tag{6}$$

Here, ω is the angular frequency of the radiated photon; γJ and $\gamma'J'$ represent, respectively, the initial and final states of the system; D is the electric dipole operator; and $\langle\gamma'J'\|D\|\gamma J\rangle$ is the reduced matrix element. The angular integrations involved in Eqs. (5) and (6) were performed using Racah algebra; the detailed expressions are given in our earlier paper [5].

III. NUMERICAL CALCULATIONS

The Hartree-Fock atomic model was used to generate the single-particle wave functions from which the radial matrix elements of Sec. II were calculated. The configuration state functions ϕ_i were constructed by angular momentum coupling and antisymmetrization. These ϕ_i served as a basis set for constructing a matrix representation for the total Hamiltonian:

$$H=\sum_i\left[-\frac{\hbar^2}{2m}\nabla_i^2-\frac{Ze^2}{r_i}-\xi(r_i)\mathbf{l}_i\cdot\mathbf{s}_i\right]+\sum_{\substack{i,j\\(i>j)}}\frac{e^2}{r_{ij}}\ .$$

Interactions among configurations belonging to the same complex were included in the calculation. The diagonal terms $\langle\phi_i|H|\phi_i\rangle$ were corrected for relativistic effects. The energy matrices were diagonalized as usual [14] to obtain corrected atomic state functions:

$$\psi_i=\sum_j C_{ij}\phi_j\ .$$

These atomic state functions were then used to calculate the transition rates and other atomic parameters of Sec. II.

IV. RESULTS AND DISCUSSION

In Table I we list the partial and total DR rate coefficients of H-like silicon, calcium, and iron. These results are extensions of data reported earlier by our group [5]. In Figs. 1, 2, and 3 we show, respectively, the partial

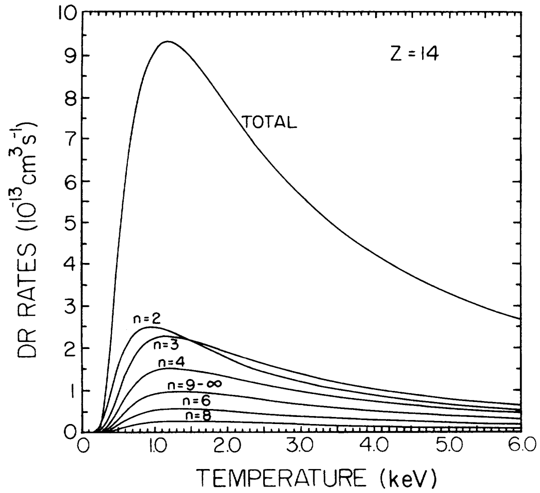

FIG. 1. Partial and total dielectronic recombination rate coefficients of H-like silicon as a function of electron temperature T_e.

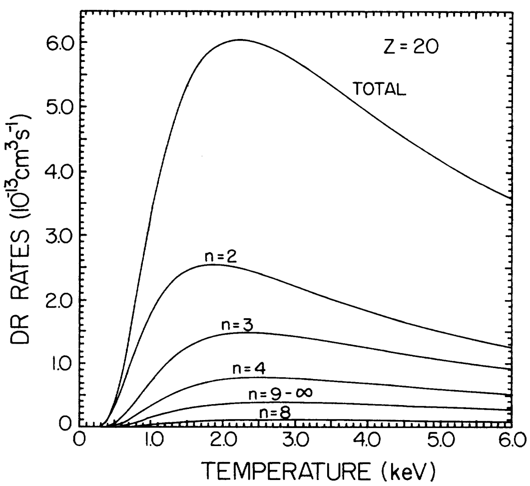

FIG. 2. Partial and total dielectronic recombination rate coefficients of H-like calcium as a function of electron temperature T_e.

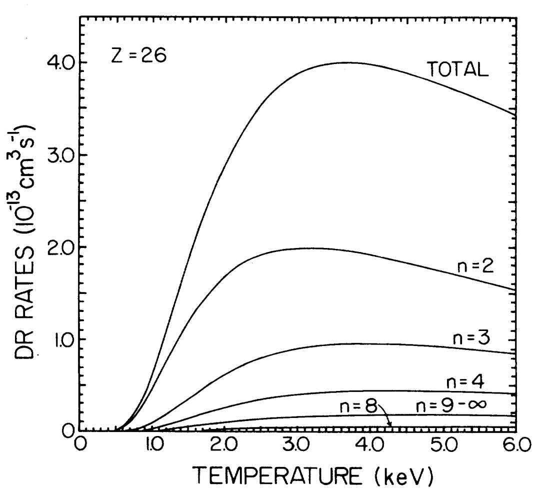

FIG. 3. Partial and total dielectronic recombination rate coefficients of H-like iron as a function of electron temperature T_e.

TABLE I. Dielectronic recombination rate coefficients for hydrogenlike silicon, calcium, and iron as a function of electron temperature T_e. The last column gives the total DR rate coefficients. Partial rate coefficients for DR processes which proceed via intermediate resonance states $2lnl'$ with $n=2$, 3, 4, 5, 6, 7, 8, and $9-\infty$ are listed, respectively, in columns 2–9. The DR rate coefficients are in units of 10^{-13} $cm^3\,s^{-1}$ and temperatures in keV.

T_e \ n	2	3	4	5	6	7	8	$9-\infty$	Total
				$Z=14$					
0.4	1.214	0.652	0.361	0.188	0.121	0.081	0.055	0.194	2.866
0.6	2.113	1.515	0.923	0.503	0.331	0.223	0.155	0.547	6.310
0.8	2.454	2.031	1.298	0.722	0.481	0.327	0.228	0.805	8.346
1.0	2.489	2.247	1.478	0.832	0.559	0.382	0.266	0.939	9.192
1.2	2.389	2.285	1.532	0.870	0.587	0.402	0.281	0.992	9.338
1.4	2.238	2.231	1.516	0.866	0.586	0.402	0.282	0.996	9.117
1.6	2.076	2.134	1.464	0.841	0.571	0.391	0.275	0.971	8.723
1.8	1.916	2.018	1.395	0.805	0.547	0.376	0.264	0.932	8.253
2.0	1.768	1.897	1.321	0.764	0.520	0.358	0.252	0.890	7.770
2.2	1.633	1.780	1.246	0.721	0.492	0.339	0.238	0.840	7.289
2.4	1.510	1.669	1.173	0.681	0.465	0.321	0.225	0.794	6.838
2.6	1.401	1.566	1.104	0.642	0.439	0.303	0.213	0.752	6.420
2.8	1.302	1.469	1.040	0.605	0.414	0.285	0.201	0.710	6.026
3.0	1.215	1.381	0.979	0.572	0.391	0.270	0.190	0.671	5.669
3.2	1.134	1.299	0.924	0.539	0.369	0.255	0.180	0.636	5.335
3.4	1.063	1.225	0.874	0.510	0.349	0.241	0.169	0.597	5.028
3.6	0.999	1.157	0.826	0.484	0.331	0.229	0.161	0.568	4.755
3.8	0.939	1.094	0.783	0.458	0.314	0.217	0.153	0.540	4.498
4.0	0.886	1.037	0.743	0.435	0.298	0.206	0.145	0.512	4.262
				$Z=20$					
0.6	0.580	0.144	0.056	0.026	0.015	0.009	0.005	0.018	0.852
0.8	1.217	0.407	0.175	0.087	0.050	0.031	0.020	0.071	2.058
1.0	1.758	0.704	0.320	0.165	0.095	0.060	0.039	0.138	3.279
1.2	2.136	0.963	0.457	0.240	0.139	0.087	0.058	0.205	4.285
1.4	2.369	1.162	0.568	0.302	0.176	0.111	0.075	0.265	5.028
1.6	2.492	1.302	0.650	0.350	0.205	0.130	0.087	0.307	5.523
1.8	2.539	1.395	0.708	0.383	0.226	0.144	0.097	0.342	5.834
2.0	2.534	1.448	0.746	0.406	0.241	0.153	0.103	0.364	5.995
2.2	2.496	1.473	0.767	0.420	0.250	0.159	0.107	0.378	6.050
2.4	2.437	1.478	0.777	0.427	0.254	0.163	0.109	0.385	6.030
2.6	2.365	1.467	0.777	0.429	0.255	0.164	0.111	0.392	5.960
2.8	2.286	1.446	0.772	0.427	0.255	0.163	0.111	0.392	5.852
3.0	2.204	1.418	0.761	0.423	0.253	0.162	0.109	0.385	5.715
3.2	2.122	1.385	0.747	0.416	0.249	0.159	0.108	0.381	5.567
3.4	2.040	1.349	0.731	0.407	0.245	0.157	0.106	0.374	5.409
3.6	1.960	1.312	0.714	0.399	0.239	0.154	0.104	0.367	5.249
3.8	1.884	1.273	0.695	0.389	0.234	0.150	0.101	0.357	5.083
4.0	1.810	1.235	0.677	0.379	0.228	0.147	0.099	0.350	4.924
4.2	1.739	1.197	0.657	0.369	0.222	0.142	0.097	0.342	4.765
4.4	1.672	1.160	0.639	0.359	0.216	0.139	0.094	0.332	4.611
4.6	1.608	1.124	0.620	0.349	0.210	0.135	0.092	0.325	4.463
4.8	1.547	1.088	0.602	0.339	0.205	0.132	0.089	0.314	4.316
5.0	1.490	1.054	0.584	0.330	0.198	0.128	0.087	0.307	4.178
5.2	1.436	1.021	0.568	0.320	0.193	0.125	0.084	0.297	4.044
5.4	1.384	0.990	0.551	0.311	0.188	0.121	0.082	0.290	3.916
5.6	1.335	0.959	0.535	0.302	0.183	0.118	0.080	0.282	3.794
5.8	1.288	0.929	0.519	0.294	0.177	0.115	0.077	0.272	3.671
6.0	1.245	0.901	0.504	0.285	0.172	0.111	0.075	0.265	3.558
				$Z=26$					
0.6	0.042	0.004	0.001	0.000	0.000	0.000	0.000	0.000	0.047
0.8	0.193	0.029	0.009	0.003	0.002	0.001	0.000	0.000	0.237

TABLE I. (*Continued*).

n / T_e	2	3	4	5	6	7	8	9–∞	Total
1.0	0.448	0.090	0.031	0.012	0.007	0.004	0.003	0.011	0.606
1.2	0.747	0.183	0.067	0.029	0.015	0.009	0.006	0.021	1.077
1.4	1.039	0.294	0.113	0.049	0.027	0.017	0.010	0.035	1.584
1.6	1.296	0.409	0.164	0.073	0.040	0.024	0.017	0.060	2.083
1.8	1.508	0.518	0.213	0.096	0.054	0.032	0.022	0.078	2.521
2.0	1.673	0.615	0.260	0.118	0.066	0.041	0.027	0.095	2.895
2.2	1.797	0.698	0.299	0.138	0.078	0.048	0.032	0.113	3.203
2.4	1.886	0.767	0.335	0.155	0.088	0.054	0.036	0.127	3.448
2.6	1.945	0.823	0.364	0.169	0.096	0.060	0.039	0.138	3.634
2.8	1.981	0.867	0.388	0.182	0.103	0.064	0.043	0.152	3.780
3.0	1.998	0.901	0.407	0.191	0.110	0.068	0.046	0.162	3.883
3.2	2.002	0.925	0.422	0.199	0.114	0.071	0.047	0.166	3.946
3.4	1.993	0.942	0.433	0.205	0.117	0.073	0.049	0.173	3.985
3.6	1.976	0.953	0.441	0.210	0.120	0.075	0.051	0.180	4.006
3.8	1.952	0.959	0.446	0.213	0.122	0.076	0.051	0.180	3.999
4.0	1.923	0.959	0.449	0.215	0.124	0.078	0.051	0.180	3.979
4.2	1.891	0.957	0.450	0.216	0.125	0.078	0.052	0.184	3.953
4.4	1.856	0.952	0.450	0.216	0.125	0.078	0.052	0.184	3.913
4.6	1.819	0.944	0.448	0.216	0.125	0.078	0.052	0.184	3.866
4.8	1.781	0.935	0.446	0.215	0.124	0.078	0.052	0.184	3.815
5.0	1.742	0.924	0.441	0.213	0.124	0.078	0.052	0.184	3.758
5.2	1.704	0.912	0.438	0.211	0.122	0.077	0.051	0.180	3.695
5.4	1.665	0.898	0.433	0.210	0.122	0.076	0.051	0.180	3.635
5.6	1.626	0.885	0.427	0.208	0.120	0.076	0.051	0.180	3.573
5.8	1.588	0.871	0.421	0.205	0.119	0.075	0.050	0.177	3.505
6.0	1.551	0.857	0.415	0.202	0.117	0.073	0.049	0.173	3.437
6.2	1.514	0.842	0.409	0.199	0.115	0.073	0.049	0.173	3.374
6.4	1.478	0.827	0.403	0.196	0.114	0.071	0.048	0.169	3.306
6.6	1.444	0.813	0.397	0.193	0.112	0.071	0.048	0.169	3.247
6.8	1.410	0.798	0.390	0.191	0.110	0.070	0.047	0.166	3.182
7.0	1.377	0.783	0.383	0.188	0.109	0.069	0.046	0.162	3.117

and total DR rate coefficients as a function of electron temperature for H-like silicon, calcium, and iron. We first compare the results from the present explicit calculations of partial DR coefficients for $n=5$, 6, 7, and 8 with those reported earlier by us [5]. In Ref. [5] DR rates were obtained explicitly in the intermediate-coupling scheme for $n=2$–4 manifolds; for $n=5$–8, a configuration average scheme was employed; and $1/n^3$ scaling was used for $n>8$. According to Table I, the value of the DR rate coefficient of H-like iron is maximum at an electron temperature of 3.6 keV. At this temperature the partial rates from the $n=2$, 3, 4, 5, 6, 7, and 8 manifolds are equal, respectively, to 1.976, 0.953, 0.441, 0.210, 0.120, 0.075, and 0.051 (in units of 10^{-13} $cm^3\,s^{-1}$). In Ref. [5] the rates for the $n=2$, 3, and 4 manifolds are listed as 1.957×10^{-13}, 0.854×10^{-13}, and 0.389×10^{-13} $cm^3\,s^{-1}$, respectively. The discrepancies for the $n=2$, 3, and 4 manifolds come from the use of a different (Hartree-Fock-Slater) atomic model in Ref. [5]. The sum of the rates for $n=5-\infty$ as reported in Ref. [5] at this temperature is 0.373×10^{-13} $cm^3\,s^{-1}$, which is a factor of 1.8 less compared to the value of 0.640×10^{-13} $cm^3\,s^{-1}$ obtained in the present calculation. The contribution from $n=5-\infty$ is about 16% of the total rate at this temperature of 3.6 keV. The total DR rate coefficient of H-like iron from the present calculation is about 11% larger than the rate coefficient reported in Ref. [5]. For H-like silicon and calcium, the total DR rates are maximum at an electron temperatures of 1.2 and 2.2 keV, respectively, with values of 9.338×10^{-13} and 6.050×10^{-13} $cm^3\,s^{-1}$, which are about 15% and 13% greater than the corresponding values of rate coefficients reported in Ref. [5].

The DR rate coefficients from the present calculation cannot be compared directly with other calculations since numerical values of DR rate coefficients are not available for the elements considered in this paper. Dubau *et al.* [7] have plotted, however, the DR rate coefficients against electron temperature for H-like iron: the maximum value of the DR rate coefficient is about 3.1×10^{-13} $cm^3\,s^{-1}$ as compared to the value of 4.0×10^{-13} $cm^3\,s^{-1}$ obtained in the present calculation. We have earlier [5,15] made a detailed comparison of satellite intensity factors and DR rate coefficients for H-like ions obtained by employing various atomic models. The present calculation does not include contributions from radiative decays leading to other autoionizing states. It has been reported by Karim and Bhalla [16] that for H-like iron such radiative cascades can increase the intensity of the prominent observable satellite lines only by about 2%. The present calculation does not include the contributions from states such as $mlnl'$, with $m,n \geq 3$. These states will predominantly decay by Auger transitions to $(m-1)l\epsilon l'$ states and will have negligible effects on the DR rate coefficients.

From Eq. (3) the DR rate coefficients should be maximum when $E_a = 3kT_e/2$, where E_a is the Auger energies for the transition $(2lnl') \rightarrow 1s + \epsilon l_c$ and T_e is the electron temperature. The position of the maxima shifts to the higher temperature accordingly with increasing Z, as is evident from Table I and Figs. 1, 2, and 3. The satellite intensity factors in Eq. (4) are large when the strengths of the radiative and nonradiative channels are comparable. For H-like ions, the Auger channels dominate in low-Z elements until about $Z=26$ when radiative and nonradiative branching ratios become comparable. The contribution of satellite intensity factors to overall DR rates is masked, however, by the dominating exponential term $\exp(-E_a/kT_e)$ in Eq. (3), and the value of DR rate coefficients is seen to decrease with Z for elements considered here.

It is interesting to apply the $1/n^3$ scaling to some of our data. According to this scheme,

$$n^3 \alpha_d(s_n \rightarrow f) = m^3 \alpha_d(s_m \rightarrow f) , \tag{7}$$

where $\alpha_d(s_n \rightarrow f)$ and $\alpha_d(s_m \rightarrow f)$ are the partial DR rate coefficients originating, respectively, from the radiative transitions $2lnl' \rightarrow f$ and $2lml' \rightarrow f$. The $1/n^3$ scaling has been found to yield better results [10,11] if $\alpha_d(s_n \rightarrow f)$ and $\alpha_d(s_m \rightarrow f)$ in Eq. (7) are replaced by corresponding partial DR rate coefficients summed over all states of each n and m. The DR rate coefficient for H-like iron at electron temperature 3.6 keV summed over all states belonging to $n=4$ is 0.441×10^{-13} $\text{cm}^3\,\text{s}^{-1}$ according to Table I. Using this value and employing Eq. (7), the DR rates for the $m=5$, 6, 7, and 8 manifolds are, respectively, 0.226×10^{-13}, 0.131×10^{-13}, 0.082×10^{-13}, and 0.055×10^{-13} $\text{cm}^3\,\text{s}^{-1}$ compared to the values of 0.210×10^{-13}, 0.120×10^{-13}, 0.075×10^{-13}, and 0.051×10^{-13} obtained by the present extensive calculations. If we apply Eq. (7) similarly to DR rate coefficients of H-like silicon at a plasma temperature of 1.2 keV, we find the DR rate coefficients for the $n=5$, 6, 7, and 8 manifolds to be 0.784×10^{-13}, 0.454×10^{-13}, 0.286×10^{-13}, and 0.191×10^{-13} $\text{cm}^3\,\text{s}^{-1}$, respectively, compared to the values of 0.870×10^{-13}, 0.587×10^{-13}, 0.402×10^{-13}, and 0.281×10^{-13} $\text{cm}^3\,\text{s}^{-1}$ of Table I. The $1/n^3$ scaling thus overestimates the DR rates in the case of H-like iron and underestimates the DR rates in the case of H-like silicon. We also see that $1/n^3$ scaling yields better estimates of DR rate coefficients for heavier elements.

V. CONCLUSION

Computations in the intermediate-coupling scheme with the inclusion of the effects of configuration interaction and spin-orbit coupling have been performed to obtain DR rate coefficients for H-like silicon, calcium, and iron. All possible intermediate resonance states $|s\rangle = |2lnl'SLJ\rangle$ with $n=2$, 3, 4, 5, 6, 7, and 8 have been considered explicitly, and the $1/n^3$ scaling has been used for $n=9-\infty$. For the elements considered here, the total DR rates from the present calculation are found to be about 14% larger than the rates obtained in our previous calculation [5] where DR rates were calculated in the intermediate-coupling scheme for $n=2-4$, in the configuration average scheme for $n=5-8$, and by $1/n^3$ scaling for $n=9-\infty$. The sum of the partial rates for $n=5-\infty$ is about 33%, 22%, and 16%, respectively, of the total DR rates for silicon, calcium, iron. The present calculation has yielded a larger value for the total DR rates for all elements considered here. In case of H-like iron, the contribution from the $n=5-\infty$ states to DR rates is found to be larger by a factor of 1.8 than the corresponding value reported in Ref. [5].

ACKNOWLEDGMENTS

This work was supported by a grant from Research Corporation and in part by the Division of Chemical Sciences, Office of Basic Energy Sciences, Office of Energy Research, U.S. Department of Energy.

[1] K. Tanaka, T. Watanabe, K. Nishi, and K. Akita, Astrophys. J. **254**, L59 (1982); G. A. Doschek, U. Feldman, and R. D. Cowan, *ibid.* **245**, 315 (1981); A. N. Parmar, J. L. Culhane, C. G. Rapley, E. Antonucci, A. H. Gabriel, and M. Loulergue, Mon. Not. R. Astron. Soc. **197**, 29 (1981).

[2] K. B. Mitchel, D. B. VanHusteyn, G. H. McCall, and P. Lee, Phys. Rev. Lett. **42**, 232 (1979); J. F. Seely, *ibid.* **42**, 1606 (1979).

[3] E. Kallne, J. Kallne, and J. E. Rice, Phys. Rev. Lett. **49**, 330 (1982).

[4] M. Bitter, S. von Goeler, S. Cohen, K. W. Hill, S. Sesnic, J. Timberlake, U. I. Safronova, L. A. Vainshtein, J. Dubau, M. Loulegue, F. Bely-Dubau, and L. Steenman-Clark, Phys. Rev. A **29**, 661 (1984).

[5] K. R. Karim and C. P. Bhalla, Phys. Rev. A **37**, 2599 (1988).

[6] K. R. Karim and C. P. Bhalla, Phys. Lett. A **116**, 172 (1986); C. P. Bhalla and K. R. Karim, Phys. Rev. A **34**, 3525 (1986); K. R. Karim and C. P. Bhalla, *ibid.* **34**, 4743 (1986).

[7] J. Dubau, A. H. Gabriel, M. Loulergue, L. Steenman-Clark, and S. Volonte, Mon. Not. R. Astron. Soc. **195**, 705 (1981).

[8] M. H. Chen, Phys. Rev. A **38**, 3280 (1988).

[9] M. S. Pindzola, N. R. Badnell, and D. C. Griffin, Phys. Rev. A **42**, 282 (1990).

[10] K. R. Karim, C. P. Bhalla, M. Ruesink, and M. Wilson, J. Phys. B **24**, L375 (1991).

[11] K. R. Karim and C. P. Bhalla, Phys. Rev. A **43**, 615 (1991).

[12] C. P. Bhalla and T. W. Tunnell, J. Quant. Spectrosc. Radiat. Transfer **32**, 141 (1984).
[13] K. R. Karim, Phys. Rev. A **32**, 2747 (1985).
[14] R. D. Cowan, *The Theory of Atomic Structure and Spectra* (University of California Press, Berkeley, CA, 1981).
[15] C. P. Bhalla and K. R. Karim, Phys. Rev. A **34**, 3525 (1986).
[16] K. R. Karim and C. P. Bhalla, Phys. Rev. A **37**, 840 (1988).